# **Aerosol Jet Printed Interconnects for Millimeter-Wave Components**

# Bryan Germann<sup>1</sup>, Alexander Ramm<sup>1</sup>, Florian Herrault<sup>2</sup>, John Hamre<sup>1</sup>, and James Feng<sup>1</sup>

<sup>1</sup>Optomec, Inc., St. Paul, Minnesota, USA <sup>2</sup>HRL Laboratories, Malibu, California, USA

#### **ABSTRACT**

As millimeter wave RF device applications expand above traditional microwave frequency bands in the global communications, automotive and Mil-Aero markets, the need to limit interconnect signal losses related to parasitic elements has never been more important. As the frequency increases, device designers are facing numerous challenges, complications, and costs when fabricating interconnects with techniques such as copper pillar bumps, wire, ribbon or wedge bonding in 3DIC packaging.

Printing conformal interconnects with Aerosol Jet® direct-write technology can offer package designers and RF engineers a new approach for optimizing interconnect transitions to active die, tailoring the loss characteristics to specific application requirements and eliminating the need to compensate for high signal transmission losses. Printed interconnects can be digitally designed into the package with a variety of metallic and dielectric materials. As these interconnects are conformally printed on the 3D surface of the package, the trace length can be minimized with zero loop height, reducing parasitic inductance to active die circuitry specifically for die on board, die in trench, or die on die with pads-up packaging configurations.

In this work, Aerosol Jet® printed interconnects with silver nanoparticle inks are compared with the gold microstrip transmission lines as well as traditional gold bond wires, for performance up to 110 GHz. We will share examples showcasing that the printed interconnects can have similar RF transmission performance to microstrip, with significantly lower loss than bondwires especially at high frequencies. We will also discuss design effects for Aerosol Jet® printed RF interconnects up to 110 GHz based on a set of results for different line heights with a given line width printed with a silver ink.

Key words: Conformal interconnects, millimeter-wave component, Aerosol Jet® printing, direct-write technology

# **INTRODUCTION**

Desired interconnects for RF components should have uniform impedance with minimal impedance discontinuities at interconnect points, to minimize signal power loss due to electromagnetic wave reflections [1]. The interconnects fabricated by the wire bonding technique tend to degrade device performance due to significant

parasitic reactance at higher frequencies especially at millimeter wave frequencies. To obtain a return loss better than -10dB, bond wires should not have lengths more than 0.1 mm at 100 GHz [2]. Although ribbon bonding or multiple wire bonding can substantially improve the interconnect performance of surface-mount millimeter-wave components by reducing parasitic inductance and discontinuities and considerable efforts using impedance compensation strategies have still been made to overcome inherent limitations and make the wire bonding viable at millimeter-wave frequencies, for its simplicity and robustness involving well-established technologies [3], its high costs are in opposition to the cost reduction goals typically associated with high volume manufacturing.

As a direct-write technology, Aerosol Jet® (AJ) printing has enabled fabrication of a variety of microelectronic devices by depositing a wide range of conducting as well as dielectric ink materials in a noncontact fashion onto 3D substrates [4, 5]. It deposits ink materials in a form of collimated high-speed mist stream consisting of ink droplets of 1 to 5  $\mu$ m allowing a long standoff between nozzle and substrate during printing, with very high resolution down to the feature size about 10  $\mu$ m [6]. Thus, the ink materials can be easily deposited onto substrates of complex 3D geometries, when the relative motion of substrate with respect to the deposition nozzle is coordinated with a motion control system driven by the toolpath generated with a CAD-CAM software interface (Figure 1).

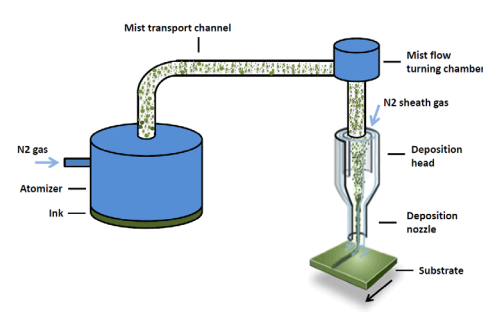


Figure 1: Schematics of the Aerosol Jet® direct-write system, consisting of an atomizer that generates mist of microdroplets of functional ink, and a mist transport-conditioning channel that delivers ink microdroplets to the deposition head, where a high-speed collimated mist jet is formed by an aerodynamic focusing nozzle with sheath gas to deposit ink material onto the substrate in a noncontact fashion

AJ printing was shown to be very effective, as an alternative to wire bond and through-silicon via (TSV) technology, for 3D interconnect applications [7, 8]. It also enables printing interconnects with significantly reduced insertion loss for high frequency applications [9, 10]. With the flexibility to vary the geometry cross-section and chose ink materials having different resistivity and CTE values, AJ printed interconnects loss performance can be tailored to the specific application requirements, enabling low-loss, low-reflection broadband transitions.

In this paper, we demonstrate an AJ direct-write process for fabricating test samples for RF signal performance evaluation. The RF signal performance of AJ printed interconnects (microstrip lines) with silver nanoparticle inks between gold pads are compared with the gold microstrip transmission lines [1] fabricated with conventional photolithography [11] as well as gold bondwires [12]. In view of the convenience with AJ printing, the AJ printed microstrip lines can have different line heights while maintaining a fixed line width, as well as different electrical resistivity values, for investigating sensitivities of RF performance to these variables.

## **TEST SAMPLE DESCRIPTION**

For the purpose of direct comparison between AJ printed interconnects and traditional bond wires against the microfabricated microstrips, a test coupon (shown in Figure 2, as an existing set of test structures re-purposed for the present work) with photolithographically patterned gold pads on a SiC wafer is used. The backside of the SiC wafer is covered with a metal ground plane. The test coupon contains five pairs of gold probe pads, one of which (2<sup>nd</sup> to the left) is open, to be connected with either an AJ printed microstrip line using a silver nanoparticle ink or a bond gold wire. The 1st one on the left and two on the right side (4th and 5th from left) are connected by a photolithographically patterned gold microstrip transmission line, and the middle one is shorted by via connection to the backside ground metal. The long microstrip (4th from left) is used in this work for comparison. This gold microstrip is 44 µm wide and 5 µm thick resulting in a characteristic impedance of 50  $\Omega$ . The distance between the gold pads of the "open" is 0.5 mm---a representative interconnect length, for an interconnect either printed by AJ or made with wire bonding.

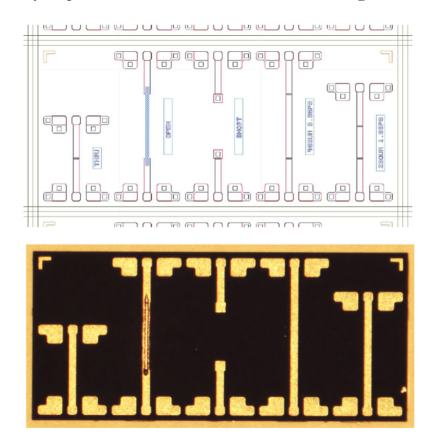


Figure 2: Test coupon for RF signal performance evaluation of AJ printed interconnect (in place, 2<sup>nd</sup> from the left) or bond wire (not shown) vs. microstrip (in place, 4<sup>th</sup> from the left)

For meaningful comparison, the AJ printed microstrip lines are targeted at a width of  $\sim$ 44  $\mu m$  (but might have different height, e.g.,  $\sim$ 4, 7, 10  $\mu m$  when printed with one, two, three passes). Figure 3 shows representative images of an AJ printed microstrip line with two pass stacking, connecting the gold probe pads at two ends.

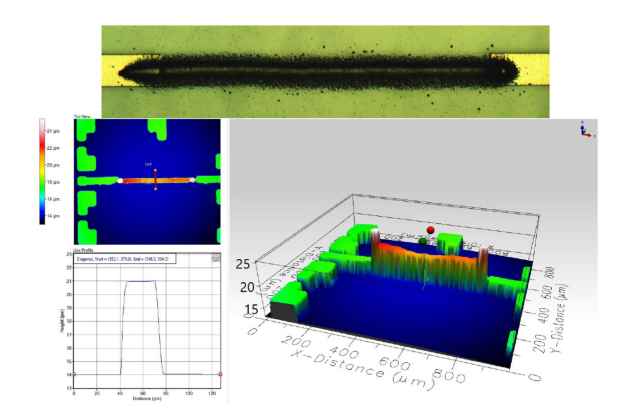


Figure 3: Microscope and white-light-interferometer images of an AJ printed (two-pass stacked) microstrip line of width ~44  $\mu m$  and height ~7  $\mu m$ , between two probe pads 0.5 mm apart

When the interconnect is made with wire bonding, instead of an AJ printed microstrip line directly on the dielectric, a loop is formed above the dielectric, the height of which is described by a so-called "loop height (as seen in Figure 4). Such a loop height creates extra parasitic inductance and a localized increase (discontinuity) in the interconnect impedance which becomes more significant at high RF frequencies [13]. If not properly compensated for, such a discontinuity will lead to undesired reflections and severe transmission loss especially at high RF frequencies.



Figure 4: A microscope image of a bond gold wire of 25.4  $\mu m$  diameter, between two probe pads 0.5 mm apart

An interconnect on the test coupon (Figures 2-4) forms a twoport network, in which the relationship between the reflected and incident voltage waves is commonly described in terms of a 2x2 scattering parameter (S-parameter) matrix [1].

The S-parameters for signal integrity are directly measured using a ground-signal-ground (GSG) probe setup connected to a vector network analyzer (Anritsu) from 1 to 110 GHz. The on-chip calibration test structures are utilized to de-embed the RF launcher from the device under test (DUT). Therefore, data for each of the AJ printed microstrip lines, bondwires, and microstrip transmission

lines on the test coupons are recorded, and compared against the theoretical values of high-frequency structure simulator (HFSS) results for an idealized microstrip transmission line.

### **AEROSOL JET PRINTING**

With AJ printing, there can be considerable degrees of freedom to create microstrip lines with different widths and heights, by varying the mist density output from the atomizer, mist flow rate and sheath gas flow rate to the deposition nozzle, nozzle orifice diameter, print speed, etc. The mist density output from the atomizer depends heavily on the atomization parameters (such as the transducer power for an ultrasonic atomizer or atomization gas flow rate for a pneumatic atomizer), as well as the ink rheological properties. The ability to vary line allows RF designers to control the impedance of interconnects much like they would do with a strip line or co-planar wave guide.

## Ink Material

In principle, any liquid material that can be atomized into a mist of microdroplets can be printed with the AJ process [4 -6]. For electrical circuit interconnects, an ink for AJ printing typically contains metal (e.g., gold, silver, copper, etc.) nanoparticles which can have metal-to-metal contact through neck growth after sintering to form an electrically conductive trace. However, the sintered metal nanoparticle inks do not have the same resistivity as the bulk metal, due to inevitable porosity which can vary significantly depending on the postprocessing conditions as well as ink formulation [14]. The resistivity value of sintered metal nanoparticle inks is often greater than 5 times of the corresponding bulk metal value, and is considered exceptionally good if less than Therefore, various electrical resistivity values can be obtained with AJ printed silver nanoparticle inks. This fact offers us an opportunity to examine the microstrip line resistivity effect on RF signal performance, by changing the type of ink and varying sintering temperature.

In this work, a silver nanoparticle ink (Loctite ECI-1011) is used for the reason of its abundant availability and simplicity of sintering in ambient condition. Slightly diluted with n-propyl acetate, it can be atomized with a pneumatic atomizer. The resistance values of printed microstrip lines can be varied from 0.1 to 0.2  $\Omega$  by changing the sintering temperature (corresponding to a resistivity about 4x that of the bulk silver).

## AJ Process Setting

For printing microstrip lines of 44 µm wide, a nozzle of 200 µm orifice diameter is used with atomization power, print speed, sheath and mist flow rates adjusted for obtaining a line height of about 3 µm in one pass. When stacked by printing two passes, the line height becomes 7 µm without significantly altering the line width (as shown in Figure 3). Because of the surface tension effect on wet ink as deposited, the cross-section profile of AJ printed lines usually do not have a rectangular shape in the strict sense; the line edge would have some slopes (unless the ink can be solidified insitu, e.g., with a UV-curable ink [6]).

It is known that the alternating electrical current density in a conductor decreases exponentially from its surface due to the nature of wave propagation. The electromagnetic wave entering a conductor is damped to 1 / e = 0.369 of its initial amplitude in a distance called the skin depth  $\delta$  [15],

$$\begin{split} \delta &= \sqrt{\frac{2 \; \rho}{\mu \; \omega}} \; \big[ \sqrt{1 + \; (\rho \omega \varepsilon)^2} + \; \rho \omega \varepsilon \big]^{- \; 1\!\!/_2} \\ &\approx \; \sqrt{\frac{2 \; \rho}{\mu \; \omega}} \; \; \text{when} \; \; \rho \; \omega \; \varepsilon \ll 1 \; \; , \end{split}$$

where p,  $\mu$ ,  $\epsilon$  denote resistivity, permeability, permittivity of the conductor (in SI units), respectively. For bulk silver,  $p=1.6 \times 10^{-8}$   $\Omega$  m,  $\mu \sim 4 \pi \times 10^{-7}$  H/m,  $\epsilon \sim 8.85 \times 10^{-12}$  F/m. At 100 GHz, we indeed still have  $p \omega \epsilon \sim 8.9 \times 10^{-8} << 1$ . Thus, the skin depth  $\delta$  for bulk silver becomes 0.2  $\mu$ m at 100 GHz (or  $\sim 0.632 \mu$ m at 10 GHz). For printed silver nanoparticle inks with a resistivity value of  $\delta$  (or 10 x) that of the bulk silver, we expect the skin depth to become  $\sim 0.45 \mu$ m (or  $0.632 \mu$ m) at 100 GHz. Thus, a printed line with height  $> 2 \mu$ m should be more than  $\delta = 0.45 \mu$ m (or  $\delta = 0.632 \mu$ m) at 100 GHz. Thus, a printed line with height  $\delta = 0.45 \mu$ m should be more than  $\delta = 0.45 \mu$ m should be more th

To produce high aspect-ratio lines (i.e., line height / width > 0.1) printing by multiple pass stacking is often an effective strategy, to provide an opportunity for solvent evaporation from the deposited ink before next pass wet ink deposition. Heating the substrate can also expedite solvent evaporation. For example, high aspect-ratio microstrip lines with heights  $\sim 4$ , 7, 10  $\mu$ m can be printed with one, two, three passes running the same toolpath over a panel of nine coupons, with about 10 seconds between each pass on substrates heated to 60 °C.

By the nature of building a printed line with numerous microdroplets with AJ printing, 'overspray' microdroplets scattered outside the edges can be visible along AJ printed lines (cf. Figure 3). Our analysis of overspray with AJ printing [16] shows that extent of overspray can be ink formulation as well as process setting dependent and typically diminishes to < 1% (in terms of percent area coverage in ImageJ analysis) beyond 30% or 40% of line width. Because the line edge formed by microdroplets is not perfectly straight and must be defined statistically as an overall area coverage  $\sim$ 50%, the overspray area coverage is always < 50% (often < 20%) even only slightly away from the line edge. Thus, conductive leakage due to percolation of two-dimensional composites [17] such as overspray is not expected likely. The fact of such a small area coverage, the capacitance produced by individual overspray spots should be negligible comparing to that of printed lines. On the other hand, the random distribution of overspray spots and related edge roughness along the printed lines are more or less statistically the same and spaced in a length scale much smaller than the RF wavelength (e.g., millimeters). The noise introduced by overspray and edge roughness in the RF interconnects cannot be more than negligible when considering other sources of process variations.

#### **RESULTS**

# Comparison of RF Signal Performance

Among the measured S-parameters, S11 represents the "return loss" due to reflection and S21 the "insertion loss" for signal transmission. In units of "dB", Figure 5 shows that the bondwire has the highest return loss (or the most reflected power) and the most insertion loss (or least transmission). The S21 values of bondwire continuously decline with increasing frequency (out of the scope of the plot), reaching -6.3 dB at 110 GHz, while the AJ printed (3 pass stacked) microstrip line has the S21 values mostly above -0.5 dB remaining close to the curves of HFSS simulation and microstrip transmission line.

There are resonant peaks in curves of the AJ printed microstrip line as well as the microstrip fabricated with the photolithography process that are not present in the simulation curve. This is due to the idealized HFSS model used for simulation of the perfect microstrip that does not include impedance deviations inherent in inevitable imperfections such as geometric roughness and noise from probe connections in the measurement system. With regard to the apparently smooth bondwire curves, the scales of the large through and return losses would render the noisy peaks relatively less obvious.

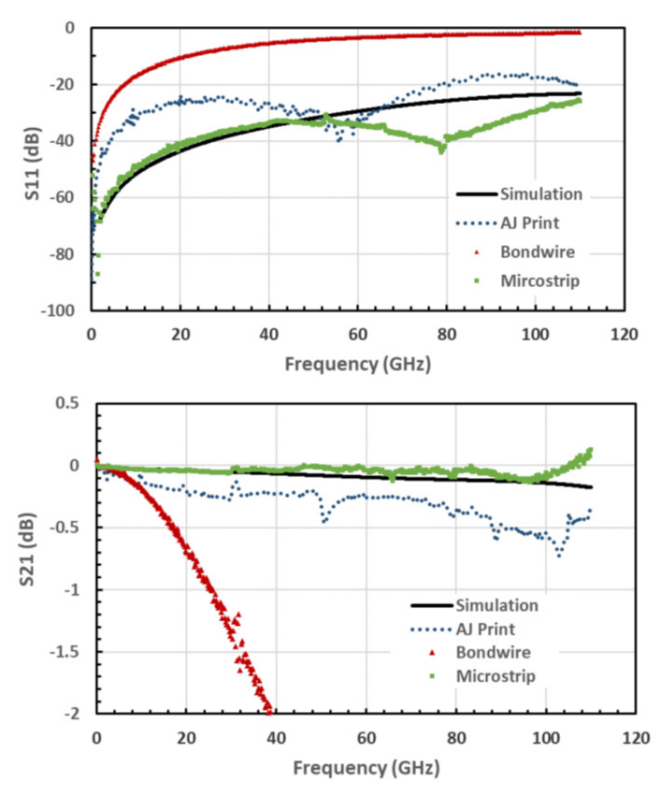


Figure 5: Curves of S11 and S21 versus RF frequency for HFSS simulation, AJ printed microstrip line, bondwire, and microstrip

# Repeatability of AJ Printed Microstrip Lines

As an additive manufacturing tool, AJ printing may have some variations in terms of the line width, line height, line profile, etc. With appropriate process control for a well-formulated ink (such as

the one used in this work), the AJ mass output (as well as line width and line height) typically meets the variation tolerance in terms of relative standard deviation (or coefficient of variation) <  $\pm 10\%$ . How such a variation tolerance affects the AJ printed interconnect performance is examined here especially at high frequencies.

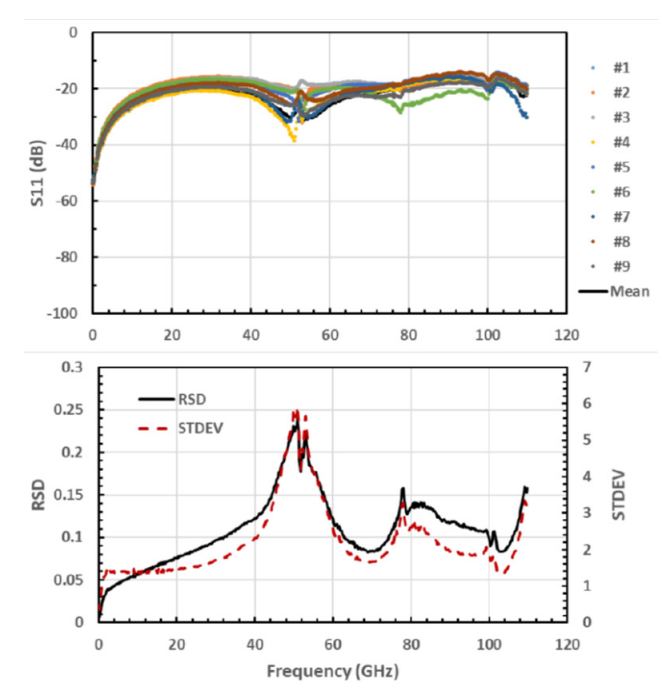


Figure 6: Measured curves of S11 versus RF frequency for 9 AJ printed microstrip lines and the corresponding relative standard deviation (RSD) as well as standard deviation (STDEV)

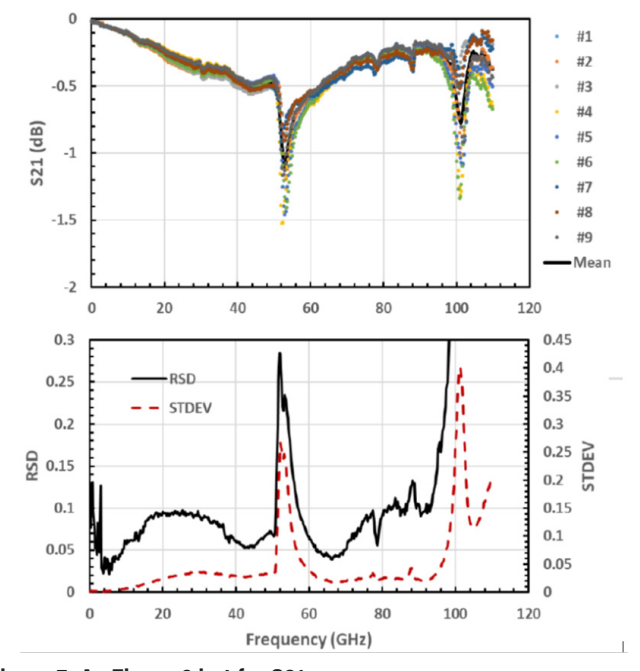


Figure 7: As Figure 6 but for S21

Figures 6 and 7 show a set of measured S11 and S21 data for nine printed (2 pass stacked) microstrip lines of height  $\sim 7~\mu m$  printed under identical process conditions. Except data around a few resonance peaks, the relative standard deviation (RSD) values in most frequency ranges are within 10% (as consistent with the current AJ process control capability of  $<\pm 10\%$  variations for mass output as well as line width and line height). Such values of standard deviation (STDEV) seem to be comparable to those reported for bondwire interconnects under 40 GHz [13].

## Effects of Microstrip Line Aspect Ratio and Resistance

There are several ways to vary the aspect ratio and resistance of microstrip lines with AJ printed inks. One variable that can easily be changed by the number of stacking layers under the same process condition is the aspect ratio and cross-section area of the printed lines. Even for lines of the same cross-section area and aspect ratio, the resistance (or resistivity) value can be varied by changing the sintering temperature. Table 1 shows the process conditions for obtaining resistance values of 0.19, 0.15, 0.098 $\Omega$  (with relative standard deviation < 10% among multiple printed lines of the same process setting) using the same silver nanoparticle ink.

Table 1: Process conditions for obtaining various resistance values of AJ printed microstrip line of width  $\sim\!44~\mu m$ 

Number of Layers	Line Height (µm)	Sintering T (degree C)	R (Ω)
2	7	150	0.19
2	7	200	0.15
3	10	350	0.098

Shown in Figure 8 is the comparison of S11 and S21 values among the three types of AJ printed microstrip lines of 0.16 and 0.23 aspect ratio, 0.19, 0.15,  $0.098\Omega$  resistance. It appears that line aspect ratio has a more noticeable effect than the resistance value.

According to electromagnetic wave theory, the interconnects can be analyzed as a lossy transmission line with characteristic impedance given by [1]

$$Z_0 = \sqrt{\frac{R + j \omega L}{G + j \omega C}} \rightarrow \sqrt{\frac{L}{C}} \text{ as } \omega \rightarrow \infty,$$

where R, L, G, C denote the series resistance, series inductance, shunt conductance, shunt capacitance per unit length of the transmission line, respectively. In practice, it is often desirable to have interconnects with characteristic impedance of 50  $\Omega$  to match the typical input and output impedance of most microwave components. For RF signals, the terms associated with angular frequency  $\omega$  in (2) typically dominate such that R and G are practically negligible in the characteristic impedance. As shown in Table 1, the AJ printed microstrip lines have R < 0.2  $\Omega$ , much

smaller than the interconnect characteristic impedance of about 50  $\Omega$ . Therefore, it is not a surprise to see little differences between the microstrip lines of the same aspect ratio but with different resistance values. However, with an ink of much higher resistivity the printed line resistance can play a considerable role in microstrip losses for D-band RF applications [18].

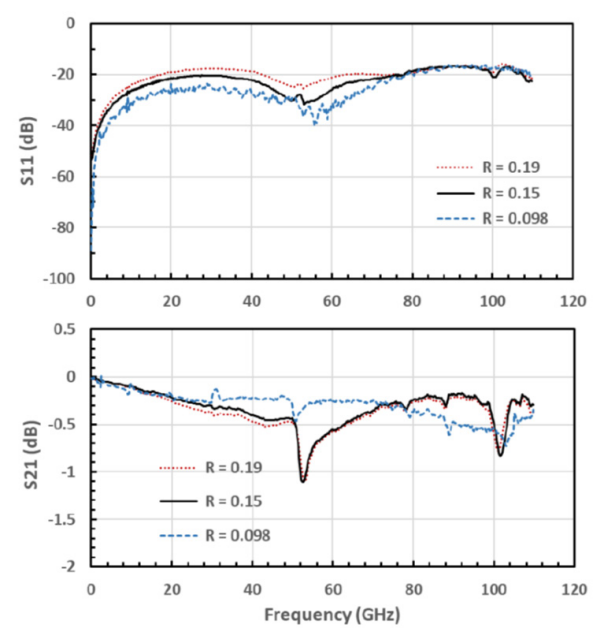


Figure 8: Effects of line aspect ratio and resistance on S11 and S21

However, geometric factors such as aspect ratio can be expected to alter the fringe fields and consequently and transmission line impedance. From Figure 8, it seems that the microstrip line of higher aspect ratio (with  $R=0.098~\Omega$ ) is more desirable for RF signal performance for relatively lower S11, higher S21, and smaller resonance peaks than that of lower aspect ratio.

## **CONCLUSIONS**

This work demonstrates that AJ printing can be used for fabricating interconnects of RF components, with the flexibility of varying the printed line geometry according to digitally designed toolpath. Comparison of RF performance is made between the straightforwardly printed silver microstrip lines by the AJ process and gold microstrip fabricated by the photolithography process, bond gold wires, against the theoretical simulation results of HFSS for an idealized microstrip. The S-parameter measurements of AJ printed microstrip lines show reasonable agreement with the HFSS theoretical results. The AJ printed interconnects can have similar RF transmission performance to microstrip, with significantly lower loss than bondwires especially at high frequencies. Unlike bondwires, the AJ printed interconnects have no loop height with a shorter length as to be beneficial for improving the interconnect performance for RF components.

To analyze the effects of line aspect ratio and resistance, microstrip lines were printed with different numbers of passes for a constant line width, and sintered at different temperatures

for different interconnect DC resistance. Our results indicates that variation of the DC resistance value of AJ printed lines have little effect on RF performance, consistent with the lossy transmission line theory that expect the characteristic impedance to be dominated by the reactance rather than resistance at high frequencies. However, the aspect ratio of AJ printed lines can have noticeable influence on their RF performance; lines of higher pile height seem to offer more desirable RF performance. This clearly illustrates the potential of AJ printing technology for producing fully optimized interconnect geometries for minimizing loss of high frequency RF packages and can offer an alternative to wire and ribbon bonding as well as prevent the need to transition to flip-chip packaging methods with copper bumps.

## **FUTURE WORK**

With the versatility and flexibility of AJ printing, interconnects of optimized geometry can be fabricated according to digitally designed toolpaths. This provides RF designers with extra tools to control the impedance of interconnects much like they would do with a microstrip or co-planar wave guide, but with the convenience for rapid-prototyping iterations. With the promising results and AJ printing capabilities demonstrated in this work, it naturally points to the future work of establishing the design rules for optimizing the AJ printed interconnect geometric pattern, aspect ratio, etc. for particular RF applications. To improve the current control capability for keeping the relative standard deviation of outputs within 10%, some feedback schemes may be implemented for tighter controls. Further development could lead to a standardized AJ printing packaging methodology for adhering to the standards for reliability common adapted in military, international telecommunications and semiconductor industry. It is also possible to incorporate AJ printing of conformal interconnects into completely additively manufactured packaging strategies like Crayton et al demonstrated in their W-band packaging strategy [19].

## **ACKNOWLEDGEMENTS**

The authors would like to thank Dr. Mike Renn for technical guidance and frequent discussions as well as the unwavering support of the colleagues of Dr. Florian Hernault on RF testing team at HRL laboratories in Malibu, California.

#### **REFERENCES**

- D. M.: Pozar, "Microwave Engineering" 4th Edition, John Wiley and Sons, 2012 ISBN 0-471-17096-8
- T. Krems, W. Haydl, H. Massler, and J. Rudiger, "Millimeter-wave performance of chip interconnections using wire bonding and flip chip", IEEE MTT-S Int. Microwave Symp. Digest (IMS), San Francisco, CA, 1996 doi: 10.1109/MWSYM.1996.508504
- V. Valenta, T. Spreng, S. Yuan, W. Winkler, V. Ziegler, D. Dancila, A. Rydberg, and H. Schumacher, "Design and experimental evaluation of compensated bondwire interconnects above 100 GHz", International Journal of Microwave and Wireless Technologies, Vol. 7(3/4), 2015, pp. 261-270 doi:10.1017/ S1759078715000070

- M. J. Renn, G. H. Marquez, B. H. King, M. Essien, and W. D. Miller, "Flow- and laser-guided direct write of electronic and biological components", in Direct-Write Technologies for Rapid Prototyping Applications: Sensors, Electronics, and Integrated Power Sources (A. Pique and D. B. Chrisey, eds), Academic Press, San Diego, CA, 2002, pp. 475-492
- N. J. Wilkinson, M. A. A. Smith, R. W. Kay, and R. A. Harris, "A review of aerosol jet printing---a non-traditional hybrid process for micro-manufacturing", International Journal of Advanced Manufacturing Technology, 2019, https://doi.org/10.1007/ s00170-019-03438-2
- J. Q. Feng and M. J. Renn, "Aerosol Jet® direct-write for microscale additive manufacturing", Journal of Micro- and Nano-Manufacturing, vol. 7(1), 2019, 011004 doi: https://doi. org/10.1115/1.4043595
- M. O'Reilly, M. J. Renn, and S. Barnes, "Aerosol jet printer as an alternative to wire bound and TSV technology for 3D intercoonect applications", Additional Confereces (Device Packaging, HiTEC, HiTEN and CICMT), 2011, (DPC):001250-001268, doi: 10.4071/2011DPC-wa11
- 8. J. A. Paulsen, M. J. Renn, K. K. Christenson, and R. Plourde, "Printing conformal electronics on 3D structures with aerosol jet technology", Future of Instrumentation International Workshop (FIIW), Gatlinburg, TN, 2012, pp. 8-9.
- F. X. Rohrl, J. Jakob, W. Bgner, R. Weigel, and S. Zorn, "Bare die connections via aerosol jet technology for millimeter wave applications", 48th European Microwave Conference (EuMC), Madrid, Spain, 2018, pp. 1033-1036, doi: 10.23919/ EuMC.2018.8541697
- C. Oakley, J. D. Albrecht, J. Papapolymerou and P. Chahal, "Low-Loss Aerosol-Jet Printed Wideband Interconnects for Embedded Devices," in IEEE Transactions on Components, Packaging and Manufacturing Technology, vol. 9, no. 11, pp. 2305-2313, Nov. 2019, doi: 10.1109/TCPMT.2019.2933792
- 11. https://en.wikipedia.org/wiki/Photolithography
- 12. M. Lapedus, "Wirebond technology rolls on," 2017, https://semiengineering.com/wirebond-technology-rolls-on/
- A. Sutono, N. G. Gafaro, J. Laskar, M. M. Tentzeris, "Experimental modeling, repeatability investigation and optimization of microwave bond wire interconnects," IEEE Trans. Adv. Packag., vol. 24(4) 2001, pp. 595-603, doi: 10.1109/6040.982850
- J. Bourassa, A. Ramm, J. Q. Feng, M. J. Renn, "Water vapor-assisted sintering of silver nanoparticle inks for printed electronics," SN Appl. Sci., vol 1 (6), 517, 2019, doi: 10.1007s42452-019-0542-0
- 15. J. D. Jackson, "Classical Electrodynamics" 2nd Edition, John Wiley and Sons, 1975 ISBN 0-471-43132-X
- J. Q. Feng, A. Ramm, M. J. Renn, "A quantitative analysis of overspray in Aerosol Jet® printing," Flexible a;nd Printed Electronics, vol 6, 2021, 045006, doi: 10.1088/2058-8585/ ac3019

 P. H. Winterfeld, L. E. Scriven, H. T. Davis, "Percolation and conductivity of random two-dimensional composites," J. Phys. C, vol. 14, 1981, 2361-2376, doi: 10.1088/0022-3719/14/17/009

- G. Gramlich, J. Hebeler, C. Bohn, U. Lemmer, T. Zwick, "Aerosol jet printed microstrip lines on polyimide for D-band," Proc. 51st Euro. Microwave Conf., London, UK, 2022, pp. 551-554
- M. T. Craton, J. D. Albrecht, P. Chahal and J. Papapolymerou, "Additive Manufacturing of a Wideband Capable W-Band Packaging Strategy," in IEEE Microwave and Wireless Components Letters, vol. 31, no. 6, pp. 697-700, June 2021, doi: 10.1109/LMWC.2021.3061614

### **BIOGRAPHIES**



Bryan Germann is an experienced mechanical engineer and product manager primarily focused on building precision manufacturing components and equipment for various end markets ranging from industrial gas turbines to medical devices, semiconductors, electronics and mil/aero. Bryan holds a BS and MS in mechanical engineering from the University of South Carolina as well as 17 patents. He began

his career working with high temperature ceramic sensors on gas turbines at GE Power, transitioning to building the automation equipment and processes to scale the instrumentation at Optomec, and finally settled into product management to develop better solutions for end use customers like him at Aerotech. As the product manager, his current work at Aerotech involves a line of high precision laser scan heads and controls, which are used for high volume cutting, drilling, micro machining and additive manufacturing applications.



Alexander Ramm is an experienced engineer with expertise in materials for electronics and in coating, printing, and dispensing processes. He worked for the Carestream Health Advanced Materials Division as a process engineer supporting the development of roll-to-roll coating of transparent conducting films. Then, he joined Optomec in 2016 as an applications

engineer, where he was responsible for designing, creating and testing proof-of-concept samples based on customer requirements while demonstrating the capabilities of Aerosol Jet® printing technology. Since 2021, he has been working at 3M as an Application Engineering Specialist, supporting structural adhesives products for consumer electronics applications. He has a B.A. in Physics from Coe College and a M.S. in Materials Science & Engineering from the University of Minnesota Twin Cities. He has published 6 peer reviewed journal articles.



Dr. Florian Herrault received the B.S. and M.S. degrees in physics and materials science from the National Institute of Applied Sciences (INSA), Toulouse, France, in 2003 and 2005, respectively, and the Ph.D. degree in electrical and electronics engineering from the University of Toulouse, Toulouse, in 2009. From 2009 to 2013, he was a Research Engineer and the Deputy Director with the MicroSensors and

MicroActuators Group, Georgia Institute of Technology, Atlanta, GA, USA. From 2013 to 2022, he worked at HRL Laboratories, LLC, Malibu, CA, USA, as a Group Leader for Advanced Packaging Solutions for mm-wave, E/O, and IR subsystems. Since 2022, he has become the co-founder and Chief Technology Officer at PseudolithIC, Inc. He has been a Senior Member of IEEE since 2014, serving on multiple IEEE committees including the ECTC and IMS conferences. He is currently the Program Chair of ECTC 2023 conference.

John Hamre is a Senior Product Development Engineer at Optomec with responsibilities for developing new equipment architecture and design of components for aerosol generation, transport and flow control in Aerosol Jet® print engines, as well as numerical simulations and consultation on electrical signal integrity related issues with Aerosol Jet® printed electronic products. He has considerable experience in architecting, designing and directing technology for electrical and mechanical industrial equipment, with extensive expertise on related electrical test systems and measurement equipment for analyzing Gbit serial data communication, signal integrity, and evaluating integrated circuit test equipment. He holds BS degrees in electrical and mechanical engineering and more than 15 patents.



Dr. James Q. Feng is a Principal Engineer of Optomec, with an extensive R&D experience in precision material placement technologies. He graduated from Tsinghua University in Beijing, before pursuing his PhD degree at University of Illinois at Urbana-Champaign in the United States. After a few years of postdoctoral researches at University of Minnesota and Oak

Ridge National Laboratory, Dr. Feng had worked at various industrial companies such as Xerox Corporation, Clear Science Corp, and Boston Scientific Corporation, prior to joining Optomec, Inc. Over years, he has published more than 60 peer-reviewed journal articles and holds more than 20 U.S. Patents.